EloR interacts with the lytic transglycosylase MltG at midcell in *Streptococcus pneumoniae* R6

Anja Ruud Winther, Morten Kjos, Marie Leangen Herigstad, Leiv Sigve Håvarstein and Daniel Straume*

Faculty of Chemistry, Biotechnology and Food Science, Norwegian University of Life Sciences, 1430 Ås, Norway.

Running title: EloR interacts with MltG at midcell.

*Corresponding author: daniel.straume@nmbu.no, +47 67232560

Key words: *Streptococcus pneumoniae*, EloR, MltG, cell division, regulation, cell wall synthesis

Abstract

The ellipsoid shape of *Streptococcus pneumoniae* is determined by the synchronized actions of the elongasome and the divisome, which have the task of creating a protective layer of peptidoglycan (PG) enveloping the cell membrane. The elongasome is necessary for expanding PG in the longitudinal direction whereas the divisome synthesizes the PG that divides one cell into two. Although there is still little knowledge about how these two modes of PG synthesis are coordinated, it was recently discovered that two RNA-binding proteins called EloR and KhpA are part of a novel regulatory pathway controlling elongation in *S. pneumoniae*. EloR and KhpA form a complex that work closely with the Ser/Thr kinase StkP to regulate cell elongation. Here, we have further explored how this regulation occur. EloR/KhpA is found at midcell, a localization fully dependent on EloR. Using a bacterial two-hybrid assay we probed EloR against several elongasome proteins and found an interaction with the lytic transglycosylase homolog MltG. By using EloR as bait in immunoprecipitation assays, MltG was pulled down confirming that they are part of the same protein complex. Fluorescent microscopy demonstrated that the Jag domain of EloR is essential for EloR's midcell localization and its interaction with MltG. Since MltG is found at midcell independent of EloR, our results suggest that MltG is responsible for recruitment of the EloR/KhpA complex to the division zone to regulate cell elongation.

Importance

Bacterial cell division has been a successful target for antimicrobial agents for decades. How different pathogens regulate cell division is, however, poorly understood. To fully exploit the potential for future antibiotics targeting cell division, we need to understand the details of how the bacteria regulate and construct cell wall during this process. Here we have revealed that the newly identified EloR/KhpA complex, regulating cell elongation in *S. pneumoniae*, forms a complex with

the essential peptidoglycan transglycosylase MltG at midcell. EloR, KhpA and MltG are conserved among many bacterial species and the EloR/KhpA/MltG regulatory pathway is most likely a common mechanism employed by many Gram-positive bacteria to coordinate cell elongation and septation.

Introduction

In order to multiply, a bacterial cell splits into two daughter cells in an intricate process involving chromosome replication and segregation, production of new cell membrane, and synthesis of new cell wall. *Streptococcus pneumoniae* is a Gram-positive species, meaning it produces a thick cell wall that surrounds and protects the cell. The major component of the cell wall is peptidoglycan (PG) which is made up of chains of polysaccharides that are cross linked with short peptide bridges. The polysaccharides consist of alternating molecules of N-acetylglucosamine (GlcNAc) and N-acetylmuramic acid (MurNAc). The cross links are made between pentapeptides attached to MurNAc (1).

S. pneumoniae has an ellipsoid shape resulting from synthesis of the PG layer by two protein complexes – the elongasome and the divisome (2, 3). As the names suggest, the elongasome is responsible for producing PG in the peripheral direction, creating the elongated shape of pneumococci. The divisome, on the other hand, is responsible for synthesizing the septal disc that divides one cell into two. The precursor for PG is made inside the pneumococcal cell, transported to the outside and incorporated into the growing PG through transglycosylation (TG) and transpeptidation (TP) reactions (1, 4). One group of enzymes performing this incorporation are the penicillin binding proteins known as PBPs. *S. pneumoniae* has six PBPs, three class A PBPs (PBP1a, PBP1b, PBP2a) that harbor both TG and TP activity, two class B PBPs (PBP2b, PBP2x) that only harbor TP activity, and PBP3, a D,D-carboxypeptidase whose activity affects the amount

of cross links in PG by removing the terminal D-Ala residues of pentapeptides (5-7). It is widely acknowledged that PBP2b is an essential part of the elongasome and PBP2x is an essential part of the divisome (8-10). The Shape Elongation Division and Sporulation (SEDS) proteins RodA and FtsW have emerged as the main TG enzymes during PG production, working alongside the TP enzymes PBP2b and PBP2x, respectively. These essential protein pairs (PBP2b/RodA and PBP2x/FtsW) are the core PG polymerizing units in *S. pneumoniae* (3, 11). The discovery that SEDS proteins are the primary TG enzymes in PG synthesis, has prompted reassessment of the role class A PBPs have in PG synthesis. Rather than being essential in building the primary PG, recent data strongly indicate that the class A PBPs are essential for maturation of newly synthesized PG, e.g. filling in gaps or mistakes left by the divisome and possibly the elongasome (12, 13). Other proteins considered to be part of the elongasome and divisome are found to be important for scaffolding, localization and regulation of PG production. One newly identified member of the elongasome is the membrane bound lytic transglycosylase MltG (14, 15). MltG in *S. pneumoniae* consists of a cytosolic domain, a transmembrane α-helix, and an extracellular catalytic domain. Several lines of evidence support that MltG is part of the elongasome: Cells depleted of MltG have reduced length, sfGFP-MltG co-localizes with elongasome proteins throughout the cell cycle, and suppressor mutations have been found in *mltG* upon deletion of the essential elongasome transpeptidase *pbp2b* demonstrating a functional link between these genes. The specific function of MltG in cell division is still unknown, but it has been proposed to release PG strands synthesized by PBP1a for cross-linking by RodA/PBP2b (15).

A particularly interesting aspect of cell wall synthesis is how PG production is regulated. By tracking the incorporation of new PG material using super-resolution fluorescence microscopy, both the elongasome and divisome PG synthesis machineries have been shown to be organized in

regularly spaced nodes in pneumococci (16), and the cells seem to elongate a short time period before septal PG synthesis is initiated (9, 17). Although several proteins are known to be involved in regulation of PG synthesis (18-24), there is little knowledge about how the temporal and spatial control of elongation and division is achieved. The eukaryotic-type Ser/Thr kinase StkP appears to play a key role in coordinating these two events (25-27). StkP phosphorylates and thereby modulates the activity of several cell division proteins, i.e. DivIVA, GpsB, MapZ, MurC, MacP and EloR (also known as Jag/KhpB) (18, 21, 24, 28-31). DivIVA and its paralogue GpsB together with StkP are important for tuning septal and peripheral PG synthesis (18, 32), and a phosphorylated MacP regulates the function of the class A PBP PBP2a (24). Furthermore, phosphorylation of MapZ (scaffolding protein for FtsZ) has been shown to be important for FtsZ ring constriction and splitting, while the effect of MurC (UDP-N-acetylmuramoyl L-alanine ligase catalyzing addition of alanine to UDP-MurNAc at an early step of the PG synthesis pathway) phosphorylation is still unclear. StkP is also important for the localization of PBP2x through interaction between StkP's PASTA domains and the pedestal and/or the transpeptidase domain of PBP2x (33).

StkP-dependent phosphorylation of EloR has also been shown to be essential in regulation of cell elongation in *S. pneumoniae* (19, 21). EloR (short for Elongasome Regulating protein) is conserved in a range of Gram-positive genera, including *Streptococcus*, *Bacillus*, *Clostridium*, *Listeria*, *Enterococcus*, *Lactobacillus* and *Lactococcus*. The protein is composed of three domains: (i) an N-terminal Jag domain, (ii) a KH-II domain and (iii) an R3H domain at its C-terminal end (Fig. 1A), but no transmembrane segment. The KH-II and R3H are both single stranded nucleic acid binding domains that usually bind RNAs, while the Jag domain has an unknown function. EloR interacts with another RNA-binding protein called KhpA (composed of one KH-II domain).

If the EloR/KhpA complex is broken, cells become shorter, consistent with loss of elongasome function, and are no longer dependent upon the essential PBP2b/RodA pair (19, 21). Point mutations inactivating the RNA-binding domains of EloR suggest that phosphorylation of EloR by StkP leads to release of bound RNA. This stimulates cell elongation in an unknown fashion (19). Interestingly, knockdown of *eloR* and *khpA* expression in the rod-shaped *Lactobacillus plantarum* also resulting in shortening of cells, suggest a conserved role for these proteins in regulating cell elongation (34). EloR and KhpA localize to the division zone of *S. pneumoniae*. While midcell localization of KhpA depends on its interaction with the KH-II domain of EloR, it is not known what directs EloR to midcell.

In this study, we employed fluorescence microscopy and protein-protein interaction assays to further explore the EloR-mediated regulation of cell elongation in *S. pneumoniae*. We show that the Jag-domain of EloR is critical for the midcell localization of this protein. Furthermore, EloR was shown to interact with the elongasome protein MltG via its Jag domain, suggesting a role of MltG in positioning EloR at midcell.

Results and discussion

The Jag domain is solely responsible for recruiting EloR to midcell

EloR consists of an N-terminal Jag domain and two C-terminal RNA-binding domains, KH-II and R3H (Fig. 1A). We and others have previously shown that EloR localizes to the division zone where it forms a complex with KhpA (20, 21). While KhpA depends on its interaction with EloR in order to localize to the division zone, it is not known how EloR finds midcell. We hypothesized that EloR must form interaction(s) with other elongasome proteins to localize correctly. The Jag domain is connected to the KH-II domain by a large linker region (134 amino acids long) with an

unknown structure and function. Since the KH-II and R3H domains bind RNA, our rationale was that the Jag-linker part of EloR would be important for its subcellular localization. We tested this by fusing full length EloR, the Jag domain, the linker region, and the Jag-linker domains to the far-red fluorescent protein mKate2, creating the strains AW407, AW408, AW410, and AW409, respectively. These fusions were expressed ectopically from an inducible promoter using the ComRS system (35). The native *eloR* gene was kept unchanged in the genome. When inducer (ComS) was supplied to the growth medium, we saw, as expected, that full length EloR fused with mKate2 (EloR-mKate2) was concentrated at midcell for 77 % of the cells investigated (Fig. 1B and C). It should be noted that we observed a background signal from the cytoplasm in most cells, suggesting that not all EloR-proteins are midcell localized. We also found that the Jag-mKate2 and the Jag-linker-mKate2 fusions concentrated at midcell for 75 % and 55 % of the cells, respectively (Fig. 1B and C). The linker-mKate2 fusion, on the other hand, did not localize to midcell (Fig. 1B), as only two percent of the linker-mKate2 cells investigated displayed a midcell fluorescent signal. These results clearly suggest that the Jag domain is solely responsible for localizing EloR to midcell. The 3D structure of the Jag domain has been solved for EloR in *Clostridium symbiosum* (PDB number 3GKU). It has a β-α-β-β fold with the α-helix laying on top of a three-stranded β-sheet. The conserved motif KKGFLG is found in the loop connecting the β2 and β3-strands (Fig. S1A). The same is true for the predicted structure of EloR from *S. pneumoniae* (Fig. S1B). We hypothesized that the conserved region (KKGFLG) could be involved in a protein-protein interaction possibly important for EloR localization. However, substitutions of several residues (K36A, K37A, F39A, and L40M) in this motif did not abrogate the midcell localization of EloR (Fig. S2).

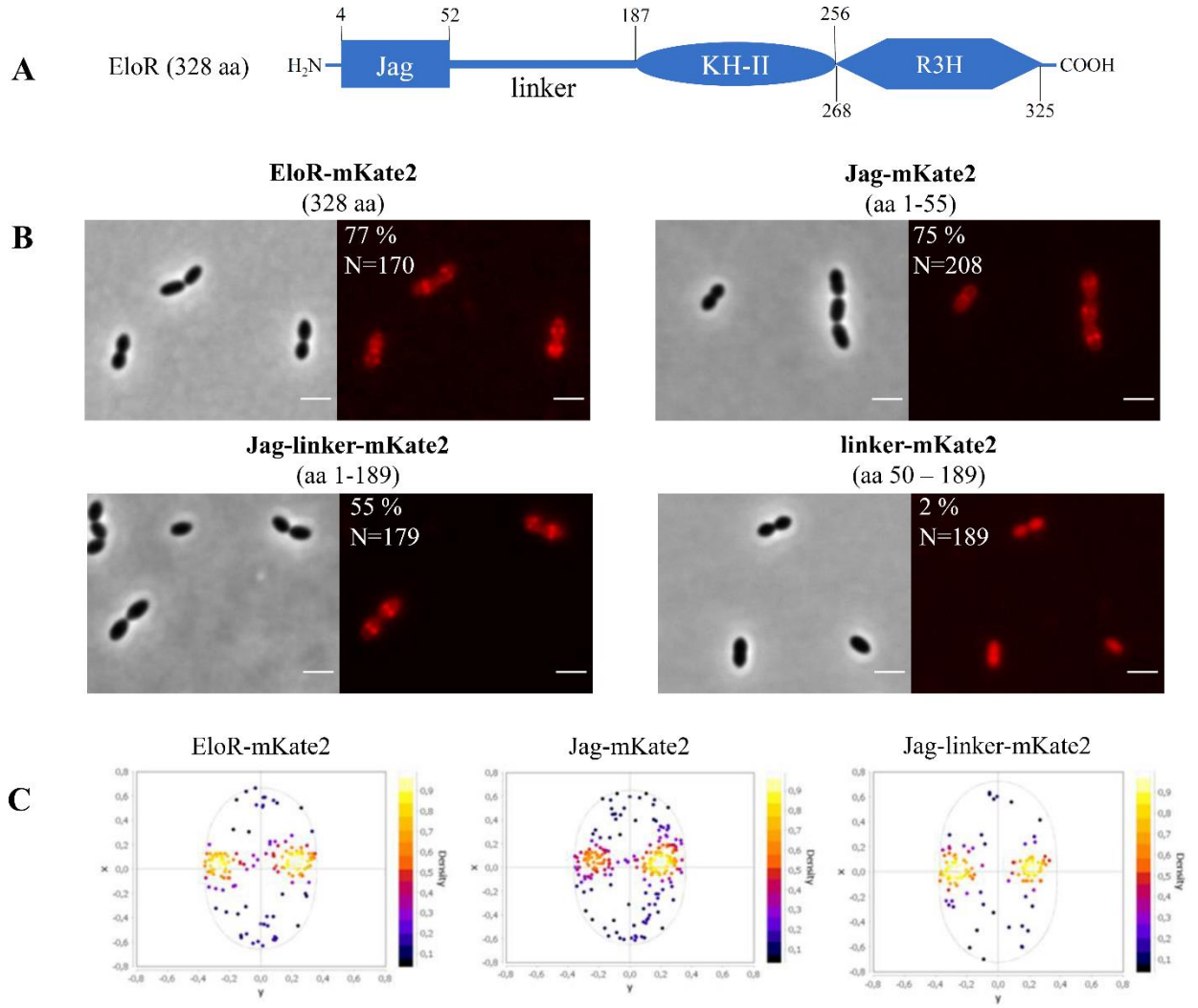

Fig. 1. The Jag domain directs EloR to midcell. A) Schematic representation of EloR, including predicted domains and domain borders. B) Micrographs showing the subcellular localization of EloR-mKate2 (AW407), Jag-mKate2 (AW408), Jag-linker-mKate2 (AW409), and linker-mKate2 (AW410). Phase contrast and corresponding fluorescence images are shown. The numbers above the micrographs indicate the amino acids of EloR utilized in the different constructs. The percentage of cells that displayed midcell localization of the mKate2-fusions are indicated, as well as the number of cells included in the analyses. Scale bars are 2 µm. C) Analysis of subcellular localization. For the strains where the majority of fusion proteins (EloR-mKate, Jag-mKate, and Jag-linker-mKate) displayed midcell localization, fluorescence maxima were detected and plotted in focus density plots using MicrobeJ (see methods). x and y in the focus density plots denote the relative length- and width-axis, respectively.

The StkP-mediated phosphorylation is not critical for EloR-localization

The results above clearly suggest that the Jag domain targets EloR to the division zone independently of the linker domain. Nevertheless, the fact that the conserved threonine (threonine 89 in *S. pneumoniae*) phosphorylated by StkP to modulate EloR activity is located in the linker domain suggests that the linker could be involved in conformational rearrangements of the EloR protein between the active and inactive form. The StkP kinase is located at midcell in *S. pneumoniae* and to explore whether this protein or the phosphorylation state affected the localization of EloR (36, 37), we analyzed the localization of EloR-mKate2 in a genetic background lacking *stkP* (Δ*stkP*::janus). However, this demonstrated that StkP is not the reason why EloR-mKate2 is concentrated at midcell, since the protein retained its localization in cells lacking *stkP* (Fig. 2A).

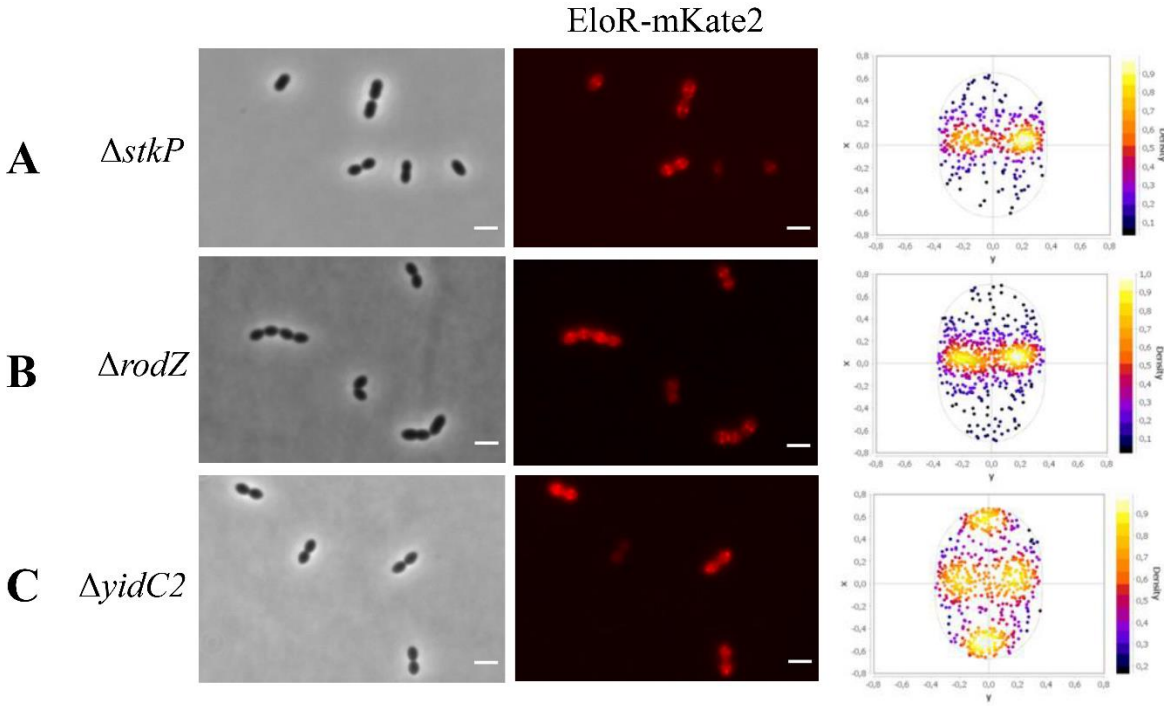

Fig. 2. EloR-mKate2 localization in different genetic backgrounds. Subcellular localization of EloR-mKate2 in A) Δ*stkP* (N = 1155), B) Δ*rodZ* (N = 1681) and C) Δ*yidC2* (N= 1280) mutants as shown by microscopy images and corresponding focus density plots of detected foci. N indicates the number of cells analyzed for each strain. x and y in the focus density plots denote the relative length - and width-axis, respectively. Scale bars are 2 µm.

Based on our localization results (Fig. 1), the linker region is not crucial for recruiting EloR to midcell. Interestingly, when aligning the amino acid sequences of EloR homologues from different Gram-positive species, the length of the linker region varies from approximately 135 amino acid residues in *S. pneumoniae* to approximately 10 residues in *Bacillus subtilis* (Fig. S3). The reason for these variations is not clear, but if the linker domain is involved in protein-protein interactions the larger linker region in the pneumococcal EloR could accommodate for more interaction partners and hence more regulatory possibilities. Why pneumococci would need this is not clear. The structural fold of the EloR linker in *S. pneumoniae* is unknown, making it particularly interesting for future studies to explore its 3D structure and the rearrangements occurring between phosphorylated EloR and the non-phosphorylated form.

EloR interacts with several proteins known to be part of the elongasome

EloR has been shown to interact with the midcell localized proteins StkP and KhpA, but these interactions did not affect the localization of EloR. In order to investigate how EloR localizes at midcell and to understand its regulatory function in cell elongation, we wanted to explore what other protein interactions EloR forms in addition to the one with KhpA and StkP. We screened our Bacterial Two-Hybrid (BACTH) library in *Escherichia coli* for possible interaction partners for EloR. The BACTH assay is based on blue (positive) and white (negative) color selection, where the blue color comes from cleavage of X-gal in the medium by β-galactosidase. Briefly, the two proteins that are tested for interaction are fused to either the T18 or T25 domain. If an interaction between the two proteins occurs, T18 and T25 reconstitute an adenylate cyclase producing cAMP which induces expression of β-galactosidase (38). EloR was probed against a range of known cell division proteins, namely PBP2b, RodA, RodZ, MreC, MreD, CozE, and MltG (Fig. 3). We also

tested YidC2 whose gene shares operon with *eloR*. YidC2 is an insertase that assists in insertion of membrane proteins into the lipid bilayer, working together with the SecYEG translocon, the signal recognition particle (SRP) and the SRP-receptor FtsY (39, 40). The presence of *yidC2* and *eloR* in one operon seems to be conserved in several species, e.g. *S. pneumoniae*, *S. mitis*, *S. oralis*, *B. subtilis*, and *Listeria monocytogenes*, indicating a functional link between the two.

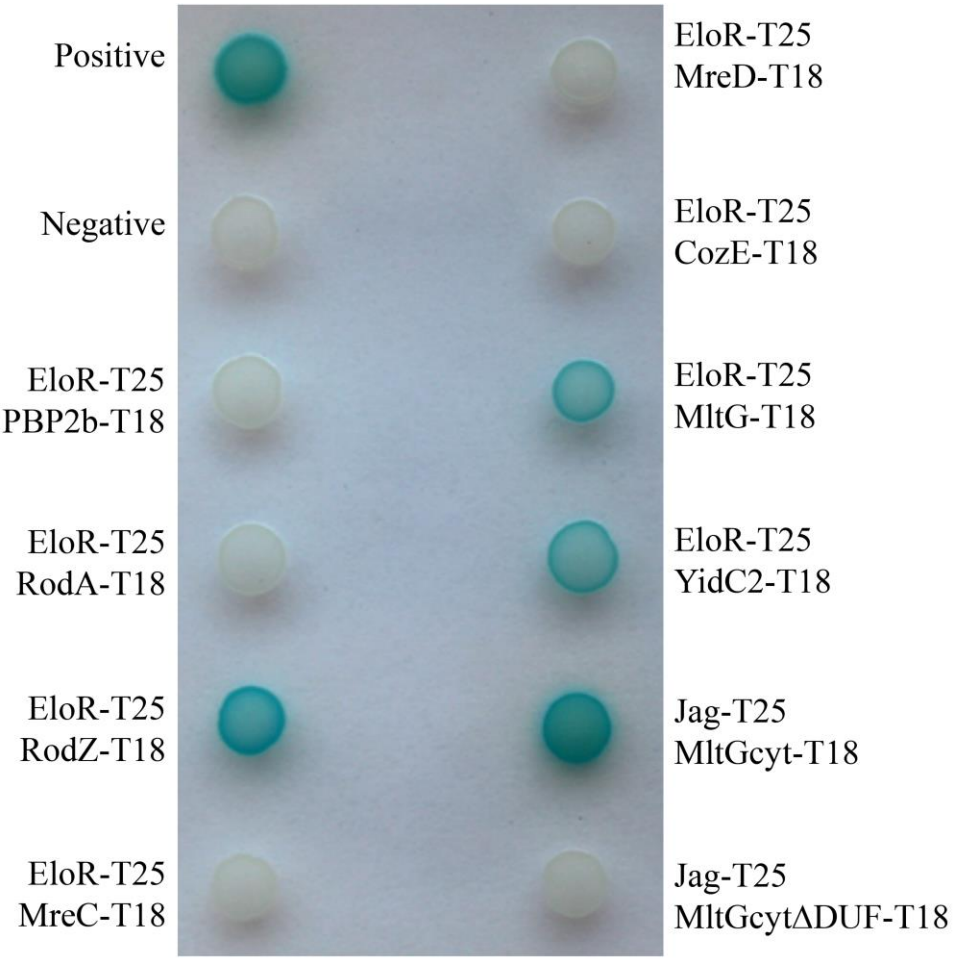

Fig. 3. Bacterial two hybrid assay probing EloR against other elongasome proteins. PBP2b, RodA, MreC, MreD, and CozE (CozEa) probed against EloR gave colorless spots of bacteria complying with no interaction between the two proteins. RodZ, MltG and YidC2 on the other hand gave blue spots when probed against EloR, suggesting that an interaction occurs. Positive and negative controls were supplied by the manufacturer (Euromedex). The Jag domain of EloR was tested against the cytosolic domain of MltG with and without the DUF domain. The interaction between the two domains were lost in the absence of the DUF domain in the cytosolic part of MltG. This indicates that the Jag domain of EloR interacts with the DUF domain of MltG.

Of all the proteins tested using BACTH, the positive hits were RodZ, YidC2 and MltG. MltG is a membrane protein predicted to be a lytic transglycosylase and is essential in *S. pneumoniae* (14). RodZ is, similar to EloR, considered to be part of the elongasome and studies in *E. coli* indicate that RodZ is important for the elongated cell shape (41). To test whether the interaction with these proteins were important for EloR localization, we analyzed EloR-mKate2 localization in cells devoid of these genes. Deletions of either *rodZ* or *yidC2*, however, did not abrogate the midcell localization of EloR-mKate2 (Fig. 2B and 2C). Interestingly, though, in the genetic background lacking *yidC2*, we now detected an accumulation of EloR-mKate2 at the poles of the cells as well as at midcell. Further investigations of the polar localization of EloR-mKate2 revealed that the polar foci of EloR-mKate2 were found in old cellular poles (Fig. S4).

EloR and MltG are part of the same complex

Since EloR was still localized at midcell when *rodZ* or *yidC2* were deleted, we hypothesized that MltG, which also has a midcell localization (15), could be important for this matter. However, MltG is essential in wild type cells making it impossible to track EloR-mKate2 in a Δ*mltG* mutant. Furthermore, we did not succeed in making an *mltG* depletion strain having EloR-mKate2 in the native *eloR* locus. Instead, to confirm the interaction between EloR and MltG *in vivo* in *S. pneumoniae* we attempted to use EloR as bait to pull down MltG. In order to do so, we constructed a mutant expressing a Flag-tagged EloR and an sfGFP-tagged MltG (strain AW447). By using resin beads tethered with α-Flag antibodies we pulled out Flag-EloR from the cell lysate as previously described by Stamsås et al., 2017. Then we looked for both Flag-EloR and sfGFP-MltG among the immunoprecipitated proteins using immunodetection and α-Flag and α-GFP antibodies (Fig. 4). Indeed, when pulling out Flag-EloR using the α-Flag resin we found that sfGFP-MltG

followed in the same fraction. Strain ds515 expressing only sfGFP-MltG was used as a negative control for a possible GFP/α-Flag interaction. In addition, to exclude a possible GFP/Flag-EloR unspecific interaction we co-expressed Flag-tagged EloR and GFP-tagged HlpA (DNA binding protein (42)) in strain AW459. When performing anti-Flag immunoprecipitation on lysates from this strain no HlpA-GFP was pulled down together with Flag-EloR.

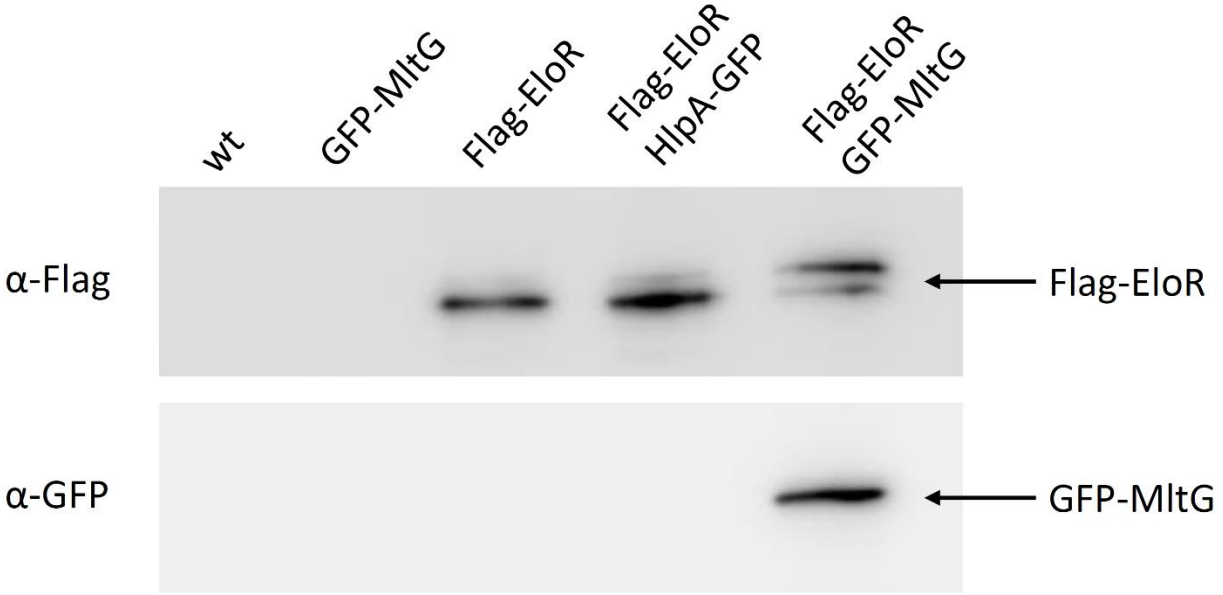

Fig. 4. Immunoblot confirming the EloR – MltG interaction. Lysates from strains RH425 (wt), ds515 (*sfgfp-mltG*), AW98 (*flag-eloR*), AW459 (*flag-eloR, hlpA-gfp*), and AW447 (*flag-eloR, sfgfp-mltG*) were incubated with resin beads tethered with α-Flag antibodies to pull down Flag-EloR. As expected, immunoprecipitated Flag-EloR was found in strain AW98, AW459 and AW447, but not in strain ds515. sfGFP-MltG was only found in immunoprecipitated fractions when it was co-expressed with a Flag-tagged EloR. The two EloR-bands visible in the blot represent the phosphorylated and unphosphorylated forms of the protein (19). All fusion proteins used in the co-IP (HlpA-GFP, Flag-EloR and GFP-MltG) have previously been shown to be stable when expressed in *S. pneumoniae* (19, 42). Uncropped versions of the immunoblots can be found in the supplementary material (Fig. S6).

The Jag domain of EloR interacts with the intracellular DUF1346 domain of MltG

The immunoprecipitation result proved that EloR is in complex with MltG *in vivo* in *S. pneumoniae*. Our BACTH results suggested that the EloR/MltG interaction is direct. To further pinpoint the EloR-MltG interaction, we performed BACTH assays with the Jag domain of EloR

(which is targeted to midcell) and the cytoplasmic part of MltG (Fig. 5). Indeed, the sole Jag domain interacted with the cytosolic part of MltG (Fig. 3). The cytosolic part of MltG mainly consists of a DUF-1346 (Domain of Unknown Function-1346) domain. When we tested the cytosolic part of MltG lacking the DUF domain against the Jag domain of EloR, the interaction between the two was lost (Fig. 3). Since MltG is located at the division zone of *S. pneumoniae* it is plausible that EloR is recruited to midcell through its interaction with MltG. Nevertheless, we cannot completely exclude the possibility that MltG is pulled down with EloR because both EloR and MltG interact with a common third protein. Further investigations (BACTH, co-IPs and cross-linking) are required to rule out this possibility.

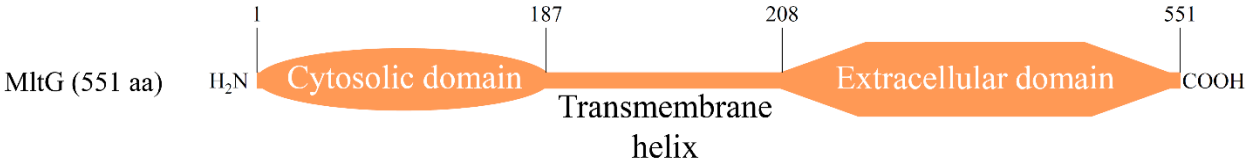

Fig. 5. Schematic representation of MltG showing the N-terminal cytosolic domain, the transmembrane helix, and the C-terminal extracellular domain. The domain boarders are indicated.

YidC2 does not affect MltG localization

Since EloR and MltG are part of the same complex, and since EloR localization was somewhat altered in the Δ*yidC2* mutant (localization to old poles, Fig. 2C and Fig. S4), we wondered whether MltG, similar to EloR, would concentrate at the cell poles as well as at midcell in the Δ*yidC2* mutant. We therefore deleted *yidC2* in the strain expressing sfGFP-MltG from the native locus. However, like in wild-type cells, sfGFP-MltG was found at midcell in the Δ*yidC2* mutant, and no polar foci were observed (Fig. S5A and S5B). Thus, in contrast to EloR, deletion of *yidC2* did not affect localization of MltG. This suggests that EloR may have additional interaction partners that need to be identified in the future, or possibly the RNA molecules it binds are concentrated at the

old poles in the Δ*yidC2* mutant. The fact that EloR displayed interaction with YidC2 in BACTH assays and that absence of YidC2 induces altered EloR localization pattern suggest a functional role of YidC2 in the EloR/KhpA regulatory pathway. Since YidC proteins assist with insertion of membrane proteins during translation it is easy to imagine that the RNA-binding protein EloR is functionally linked to this process e.g. controlling the expression of one or several elongasome proteins. To unravel this would require additional research. The localization of sfGFP-MltG was not affected by the loss of *eloR*, as previously reported (19) and seen in Fig. S5C.

Concluding remarks

It has previously been shown that knocking out the essential *pbp2b* results in suppressor mutations in *mltG, eloR* or *khpA* relieving the requirement of the elongasome in *S. pneumoniae* (15, 19). The current finding that EloR and MltG interact therefore corroborate that MltG and EloR are part of the same regulatory pathway. KhpA is also part of this complex since it has been shown previously to interact directly with EloR at the division zone (20, 21). In sum we can conclude that MltG, EloR and KhpA form a protein complex at the division zone, which regulates the elongasome on command from StkP. The relationship between EloR/KhpA and MltG is unknown. We have previously speculated that the expression level of MltG is controlled via the RNA-binding capacity of EloR/KhpA. This, however, turned out to be wrong as the amount of MltG in a wild type background and in a Δ*eloR* mutant are similar (19). Another hypothesis is that the EloR/KhpA complex regulates the activity of MltG. MltG in *E. coli* have been shown to possess endolytic transglycosylase activity, i.e. breaking glycosidic bonds within a glycan strand (14). Structural modelling and site directed mutagenesis of the active site of the pneumococcal MltG suggest that it has the same muralytic activity (15). Interestingly, it seems that MltG is not tolerated in neither *E. coli* nor *S. pneumoniae* mutants with compromised PG synthases (14, 15, 43), suggesting that

the muralytic activity of MltG becomes lethal if a weaker PG layer is produced due to inefficient PG synthesis. In *S. pneumoniae* MltG is most likely activated by EloR/KhpA since deletions of EloR and KhpA suppress the toxic effect MltG has in Δ*pbp2b*/Δ*rodA* mutants. *E. coli*, on the other hand, does not express EloR and it has an MltG lacking the cytoplasmic domain found to interact with EloR in *S. pneumoniae*. Hence, MltG must be regulated through a different mechanism in this species. It has been hypothesized that MltG releases glycan strands made by both class A and B PBPs so that they can be cross linked to new PG by the divisome and elongasome (15, 43). While this intriguing model might be proven correct, recent discoveries suggesting that class A PBPs are not involved in the primary PG synthesis (elongasome and divisome) but rather function to repair, mature or strengthen newly synthesized PG combined with the fact that MltG is associated with the elongasome (12, 13, 15), lead us to suggest an alternative model: MltG may work together with amidases to open the PG layer so that PBP2b/RodA can add new PG to the existing layer and hence elongate the dividing cell (Fig. 6). MltG must therefore be strictly regulated to avoid uncontrolled damage to the PG layer when PG synthase activity is reduced. The present study has shown just how important the MltG levels in the cells are: adjusting the expression level of MltG from an inducible promoter has proved to be difficult, and hence subsequent genetic changes to *eloR*, which is part of the same pathway, is not possible. Based on the data presented here, the EloR/KhpA complex appears to play a key role in regulation of MltG. Since inactivation of the RNA-binding domains of EloR gives the same phenotype as inactivation of the catalytic domain of MltG (PBP2b/RodA becomes redundant) (15, 19), one could speculate that the EloR/KhpA complex modulates the activity of MltG via the RNA-binding domains. Another possibility is that EloR regulates the MltG activity directly by interacting with other cell division proteins. This must be confirmed or rejected by further experimental evidence.

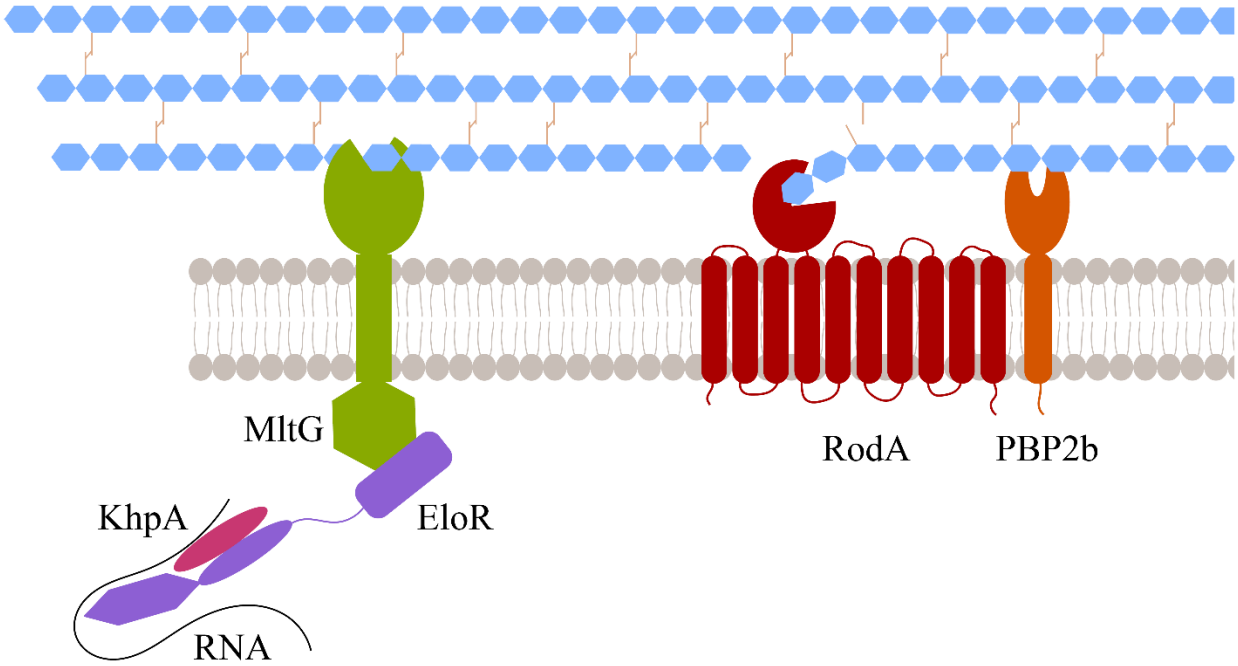

Fig. 6. Modell of MltG/EloR/KhpA function. The communication between EloR/KhpA/RNA and MltG allows for a controlled opening of the PG. These openings are utilized by PBP2b/RodA to insert new PG in the lateral direction of the cell and in this way elongate the cell.

Methods

Bacterial strains, cultivation and transformation. All bacterial strains used in this work are listed in Table 1. All *E. coli* strains were grown in liquid LB broth with shaking or on LB agar plates at 30°C or 37°C. When necessary, the following antibiotic concentrations were used: 100 µg/ml ampicillin and 50 µg/ml kanamycin. Transformation of *E. coli* was performed with heat shock at 42°C for 30 seconds. All *S. pneumoniae* strains were grown in C-medium (44) without shaking or on Todd-Hewitt (TH) agar plates in an oxygen-depleted chamber using AnaeroGenTM bags from Oxoid at 37°C. Concentrations of 200 µg/ml streptomycin, 400 µg/ml kanamycin or 2 µg/ml chloramphenicol were employed when necessary. When introducing genetic changes,

natural transformation was utilized. Exponentially growing cells were diluted to an OD_{550} of 0.05-0.1 and grown for two hours with 100-200 ng of the transforming DNA and 250 ng/ml CSP (final concentration) added to the growth medium. Thirty µl of the transformed cell cultures were plated on TH agar plates with the appropriate antibiotic and incubated at 37°C overnight.

DNA constructs. All primers used in this study are listed in Table S1. DNA constructs used to transform *S. pneumoniae* were made using overlap extension PCR (45). In short, in order to create deletion mutants, approximately 1000 bp sequence upstream and downstream of the gene in question were amplified and fused with the 5' end and 3' end of the Janus cassette (46), respectively. The same flanking regions were then used to replace the Janus cassette with an alternative DNA sequence (47). Constructs used to produce BACTH plasmids were amplified from *S. pneumoniae,* cleaved with restriction enzymes (XbaI and EcoRI from New England BioLabs), and ligated into the preferred plasmid using Quick ligase (New England BioLabs). The plasmids used in this study are listed in Table 1. All constructs were verified with DNA sequencing.

Bacterial two hybrid assay. Bacterial two hybrid (BACTH) assays are based on the two tags T18 and T25 that make up the catalytic domain of *Bordetella pertussis* adenylate cyclase (CyaA). In order to test whether two proteins interact, their genes are cloned in frame with one tag each and co-expressed in *E. coli* BTH101 cells (*cyaA*-). If the two proteins interact, T18 and T25 are brought into close proximity to make up an active CyaA catalytic domain. This results in cAMP production which induces expression of *lacZ* (β-galactosidase). β-galactosidase cleaves X-gal, resulting in blue bacteria on X-gal containing agar plates. In instances where the two tested proteins do not interact, no β-galactosidase is expressed, and the bacteria remain white. The BACTH experiments were performed as described by the manufacturer (Euromedex). The genes encoding our proteins of interest were cloned in reading frame with either the T18 or T25 encoding gene in the plasmids

pUT18, pUT18C, pKNT25 and pKT25. The plasmids were then transformed into *E. coli* XL1-Blue cells, then isolated and sequenced. In order to test the interaction between two proteins, they were co-expressed with one tag (T18, T25) each in *E. coli* BTH101 cells. After overnight incubation of transformants, five random colonies were picked, grown to exponential phase, and spotted (2 µl) onto LB agar plates containing ampicillin (100 µg/ml), kanamycin (50 µg/ml), IPTG (0.5 mM) and X-gal (40µg/ml). After overnight incubation at 30°C the results were documented.

Co-immunoprecipitation and western blotting. Co-IP was performed using ANTI-FLAG® M2 affinity gel (Sigma-Aldrich). *S. pneumoniae* strains were grown to OD_{550} = 0.3 and lysed with 1 ml lysis buffer (50 mM Tris HCl, pH 7.4, 150 mM NaCl, 1 mM EDTA, 1% Triton X-100) by triggering the endogenous pneumococcal autolysin LytA at 37°C for 5 minutes. The lysate was incubated with 40 µl ANTI-FLAG® M2 affinity gel with gentle rotation at 4°C overnight. After washing the affinity gel three times with 500 µl TBS, SDS sample buffer was added and the samples were incubated at 95°C for 10 minutes. Proteins from eight µl of each sample were separated in a 12 % SDS PAGE gel. After electrophoresis the separated proteins were electroblotted onto a PVDF membrane using a Trans-Blot Turbo Transfer System (Bio-Rad) with a standard protocol for seven minutes. Finally, Flag-tagged proteins were detected as previously described by Stamsås et al, 2017. GFP-tagged proteins were detected with Chromotek rabbit polyclonal antibody for GFP, using the same protocol as above and dilutions as recommended by the manufacturer.

Phase contrast and fluorescent microscopy. Cells were prepared for microscopic imaging by growing them to OD_{550} = 0.4, then diluting the culture to OD_{550} = 0.1 and grown for another hour prior to microscopy. When relevant, 2 µM ComS inducer was added. Proteins fused with the fluorescent mKate2 were visualized as previously described (19) using a Zeiss AxioObserver with

ZEN Blue software, an ORCA-Flash 4.0 V2 Digital CMOS camera (Hamamatsu Photonics), and a 100x phase-contrast objective. An HXP 120 Illuminator (Zeiss) was used as a fluorescence light source. Images were prepared and analyzed using the ImageJ software with the MicrobeJ plugin (48). For subcellular localization analysis, the "Maxima" function in MicrobeJ was used to define fluorescence maxima within cells, and the average subcellular localization of these maxima were plotted using the "XYCellDensity" plot (focus density plots) in MicrobeJ.

Acknowledgements. This work was supported by grants from the Research Council of Norway (project numbers 296906, 250976).

Table 1. Bacterial strains and plasmids.

***S. pneumoniae* strains**	**Relevant characteristics**	**Source**
R704	R6 derivative, *comA*::*ermAM*; Ery^r	J. P. Claverys
RH425	R704, but streptomycin resistant; Ery^r, Sm^r	(49)
SPH131	Δ*comA*, P1*::*P_{comR}*::comR*, P_{comX}*::Janus*; Ery^r Kan^r	(35)
AW407	Δ*comA*, P1*::*P_{comR}*::comR*, P_{comX}*::eloR-mKate2*; Ery^r Sm^r	This work
AW408	Δ*comA*, P1*::*P_{comR}*::comR*, P_{comX}*::jag-mKate2*; Ery^r Sm^r	This work
AW409	Δ*comA*, P1*::*P_{comR}*::comR*, P_{comX}*::jag-linker-mKate2*; Ery^r Sm^r	This work
AW410	Δ*comA*, P1*::*P_{comR}*::comR*, P_{comX}*::linker-mKate2*; Ery^r Sm^r	This work
AW420	Δ*comA*, P1*::*P_{comR}*::comR*, P_{comX}*::eloR*^{K36A}*-mKate2*; Ery^r, Sm^r	This work
AW424	Δ*comA*, P1*::*P_{comR}*::comR*, P_{comX}*::eloR*^{K37A}*-mKate2*; Ery^r, Sm^r	This work
AW425	Δ*comA*, P1*::*P_{comR}*::comR*, P_{comX}*::eloR*^{F39A}*-mKate2*; Ery^r, Sm^r	This work
AW426	Δ*comA*, P1*::*P_{comR}*::comR*, P_{comX}*::eloR*^{L40M}*-mKate2*; Ery^r, Sm^r	This work
AW453	Δ*comA*, P1*::*P_{comR}*::comR*, P_{comX}*::eloR-mKate2*, Δ*stkP::janus*; Ery^r, Km^r	This work
AW415	Δ*comA*, P1*::*P_{comR}*::comR*, P_{comX}*::eloR-mKate2*, Δ*yidC2::janus*; Ery^r, Km^r	This work

AW417	Δ*comA*, P1*::*P$_{comR}$*::comR*, P$_{comX}$*::eloR-mKate2*, Δ*rodZ::janus*; Ery^r, Km^r	This work
AW447	Δ*comA, m(sf)gfp-mltG, flag-eloR*; Ery^r Sm^r	This work
AW459	Δ*comA, flag-eloR, hlpA-gfp-chloramphenicol*; Ery^r, Sm^r, Cam^r	This work
DS515	Δ*comA, m(sf)gfp-mltG*; Ery^r, Sm^r	(19)
AW98	Δ*comA, flag-eloR*; Ery^r, Sm^r	(19)
MH43	Δ*comA, m(sf)gfp-mltG*; Δ*yidC2::janus*; Ery^r, Km^r	This work
SPH472	Δ*comA, m(sf)gfp-mltG*; Δ*eloR::janus*; Ery^r, Km^r	(19)
***E. coli* strains**		
XL1-Blue	Host strain	Agilent Technologies
BTH101	BACTH expression strain, *cya-*	Euromedex
Plasmids		
pKT25	Plasmid used in BACTH analysis	Euromedex
pKNT25	Plasmid used in BACTH analysis	Euromedex
pUT18C	Plasmid used in BACTH analysis	Euromedex
pUT18	Plasmid used in BACTH analysis	Euromedex
pKNT25-eloR	T25 domain fused to the C-terminus of EloR	(19)
pKT25-jag	T25 domain fused to the N-terminus of the Jag domain of EloR	This work
pUT18C-mltG	T18 domain fused to the N-terminus of MltG	(19)
pUT18C-mltG$_{cyt}$	T18 domain fused to the N-terminus of the cytoplasmic domain of MltG	This work
pUT18C-mltG$_{cyt\Delta DUF}$	T18 domain fused to the N-terminus of the cytoplasmic domain of MltG without DUF	This work
pUT18C-pbp2b	T18 domain fused to the N-terminus of PBP2b	(50)
pUT18C-rodA	T18 domain fused to the N-terminus of RodA	(50)
pUT18C-rodZ	T18 domain fused to the N-terminus of RodZ	(19)
pUT18C-mreC	T18 domain fused to the N-terminus of MreC	(19)
pUT18C-mreD	T18 domain fused to the N-terminus of MreD	This work
pUT18-cozE	T18 domain fused to the C-terminus of CozE	(50)
pUT18-yidC2	T18 domain fused to the C-terminus of YidC2	This work

References

1. Vollmer W, Blanot D, De Pedro MA. 2008. Peptidoglycan structure and architecture. FEMS microbiology reviews 32:149-167.

2. Pinho MG, Kjos M, Veening J-W. 2013. How to get (a) round: mechanisms controlling growth and division of coccoid bacteria. Nature reviews microbiology 11:601.
3. Cho H, Wivagg CN, Kapoor M, Barry Z, Rohs PD, Suh H, Marto JA, Garner EC, Bernhardt TG. 2016. Bacterial cell wall biogenesis is mediated by SEDS and PBP polymerase families functioning semi-autonomously. Nature microbiology 1:16172.
4. Typas A, Banzhaf M, Gross CA, Vollmer W. 2012. From the regulation of peptidoglycan synthesis to bacterial growth and morphology. Nature Reviews Microbiology 10:123.
5. Sauvage E, Kerff F, Terrak M, Ayala JA, Charlier P. 2008. The penicillin-binding proteins: structure and role in peptidoglycan biosynthesis. FEMS microbiology reviews 32:234-258.
6. Zapun A, Vernet T, Pinho MG. 2008. The different shapes of cocci. FEMS microbiology reviews 32:345-360.
7. Morlot C, Pernot L, Le Gouellec A, Di Guilmi AM, Vernet T, Dideberg O, Dessen A. 2005. Crystal structure of a peptidoglycan synthesis regulatory factor (PBP3) from *Streptococcus pneumoniae*. Journal of Biological Chemistry 280:15984-15991.
8. Berg KH, Stamsås GA, Straume D, Håvarstein LS. 2013. Effects of low PBP2b levels on cell morphology and peptidoglycan composition in *Streptococcus pneumoniae* R6. Journal of bacteriology 195:4342-4354.
9. Tsui HCT, Boersma MJ, Vella SA, Kocaoglu O, Kuru E, Peceny JK, Carlson EE, VanNieuwenhze MS, Brun YV, Shaw SL. 2014. Pbp2x localizes separately from Pbp2b and other peptidoglycan synthesis proteins during later stages of cell division of *Streptococcus pneumoniae* D39. Molecular microbiology 94:21-40.
10. Perez AJ, Cesbron Y, Shaw SL, Villicana JB, Tsui H-CT, Boersma MJ, Ziyun AY, Tovpeko Y, Dekker C, Holden S. 2019. Movement dynamics of divisome proteins and PBP2x: FtsW in cells of *Streptococcus pneumoniae*. Proceedings of the National Academy of Sciences 116:3211-3220.

11. Meeske AJ, Riley EP, Robins WP, Uehara T, Mekelanos JJ, Kahne D, Walker S, Kruse AC, Bernhardt TG, Rudner DZ. 2016. SEDS proteins are a widespread family of bacterial cell wall polymerases. Nature.

12. Straume D, Piechowiak KW, Olsen S, Stamsås GA, Berg KH, Kjos M, Heggenhougen MV, Alcorlo M, Hermoso JA, Håvarstein LS. 2020. Class A PBPs have a distinct and unique role in the construction of the pneumococcal cell wall. Proceedings of the National Academy of Sciences 117:6129-6138.

13. Vigouroux A, Cordier B, Aristov A, Oldewurtel E, Özbaykal G, Chaze T, Matondo M, Bikard D, van Teeffelen S. 2020. Class-A penicillin binding proteins do not contribute to cell shape but repair cell-wall defects. eLife 9:e51998

14. Yunck R, Cho H, Bernhardt TG. 2016. Identification of MltG as a potential terminase for peptidoglycan polymerization in bacteria. Molecular microbiology 99:700-718.

15. Tsui HCT, Zheng JJ, Magallon AN, Ryan JD, Yunck R, Rued BE, Bernhardt TG, Winkler ME. 2016. Suppression of a deletion mutation in the gene encoding essential PBP2b reveals a new lytic transglycosylase involved in peripheral peptidoglycan synthesis in *Streptococcus pneumoniae* D39. Molecular microbiology 100:1039-1065.

16. Perez AJ, Boersma MJ, Bruce KE, Lamanna MM, Shaw SL, Tsui HCT, Taguchi A, Carlson EE, VanNieuwenhze MS, Winkler ME. 2020. Organization of Peptidoglycan Synthesis in Nodes and Separate Rings at Different Stages of Cell Division of *Streptococcus pneumoniae*. Molecular Microbiology.

17. Wheeler R, Mesnage S, Boneca IG, Hobbs JK, Foster SJ. 2011. Super-resolution microscopy reveals cell wall dynamics and peptidoglycan architecture in ovococcal bacteria. Molecular microbiology 82:1096-1109.

18. Fleurie A, Manuse S, Zhao C, Campo N, Cluzel C, Lavergne J-P, Freton C, Combet C, Guiral S, Soufi B, Kuru E, VanNieuwenhze MS, Brun YV, Di Guilmi A-M, Claverys J-P, Galinier A,

Grangeasse C. 2014. Interplay of the serine/threonine-kinase StkP and the paralogs DivIVA and GpsB in pneumococcal cell elongation and division. PLoS genetics 10:e1004275.

19. Stamsås GA, Straume D, Ruud Winther A, Kjos M, Frantzen CA, Håvarstein LS. 2017. Identification of EloR (Spr1851) as a regulator of cell elongation in *Streptococcus pneumoniae*. Molecular microbiology 105:954-967.

20. Winther AR, Kjos M, Stamsås GA, Håvarstein LS, Straume D. 2019. Prevention of EloR/KhpA heterodimerization by introduction of site-specific amino acid substitutions renders the essential elongasome protein PBP2b redundant in *Streptococcus pneumoniae*. Scientific Reports 9:3681.

21. Zheng JJ, Perez AJ, Tsui HCT, Massidda O, Winkler ME. 2017. Absence of the KhpA and KhpB (JAG/EloR) RNA-binding proteins suppresses the requirement for PBP2b by overproduction of FtsA in *Streptococcus pneumoniae* D39. Molecular microbiology 106:793-814.

22. Fenton AK, El Mortaji L, Lau DT, Rudner DZ, Bernhardt TG. 2017. Erratum: CozE is a member of the MreCD complex that directs cell elongation in *Streptococcus pneumoniae*. Nature microbiology 2:17011.

23. Stamsås GA, Restelli M, Ducret A, Freton C, Garcia PS, Håvarstein LS, Straume D, Grangeasse C, Kjos M. 2020. A CozE Homolog Contributes to Cell Size Homeostasis of *Streptococcus pneumoniae*. Mbio 11.

24. Fenton AK, Manuse S, Flores-Kim J, Garcia PS, Mercy C, Grangeasse C, Bernhardt TG, Rudner DZ. 2018. Phosphorylation-dependent activation of the cell wall synthase PBP2a in *Streptococcus pneumoniae* by MacP. Proceedings of the National Academy of Sciences 115:2812-2817.

25. Manuse S, Fleurie A, Zucchini L, Lesterlin C, Grangeasse C. 2015. Role of eukaryotic-like serine/threonine kinases in bacterial cell division and morphogenesis. FEMS microbiology reviews 40:41-56.

26. Fleurie A, Cluzel C, Guiral S, Freton C, Galisson F, Zanella-Cleon I, Di Guilmi AM, Grangeasse C. 2012. Mutational dissection of the S/T-kinase StkP reveals crucial roles in cell division of *Streptococcus pneumoniae*. Molecular microbiology 83:746-758.

27. Beilharz K, Nováková L, Fadda D, Branny P, Massidda O, Veening J-W. 2012. Control of cell division in *Streptococcus pneumoniae* by the conserved Ser/Thr protein kinase StkP. Proceedings of the National Academy of Sciences 109:E905-E913.

28. Fleurie A, Lesterlin C, Manuse S, Zhao C, Cluzel C, Lavergne J-P, Franz-Wachtel M, Macek B, Combet C, Kuru E. 2014. MapZ marks the division sites and positions FtsZ rings in *Streptococcus pneumoniae*. Nature 516:259-262.

29. Holečková N, Doubravová L, Massidda O, Molle V, Buriánková K, Benada O, Kofroňová O, Ulrych A, Branny P. 2015. LocZ is a new cell division protein involved in proper septum placement in *Streptococcus pneumoniae*. MBio 6:e01700-14.

30. Falk SP, Weisblum B. 2013. Phosphorylation of the *Streptococcus pneumoniae* cell wall biosynthesis enzyme MurC by a eukaryotic-like Ser/Thr kinase. FEMS microbiology letters 340:19-23.

31. Ulrych A, Holečková N, Goldová J, Doubravová L, Benada O, Kofroňová O, Halada P, Branny P. 2016. Characterization of pneumococcal Ser/Thr protein phosphatase *phpP* mutant and identification of a novel PhpP substrate, putative RNA binding protein Jag. BMC microbiology 16:247.

32. Rued BE, Zheng JJ, Mura A, Tsui HCT, Boersma MJ, Mazny JL, Corona F, Perez AJ, Fadda D, Doubravová L. 2017. Suppression and synthetic-lethal genetic relationships of Δ*gpsB* mutations indicate that GpsB mediates protein phosphorylation and penicillin-binding protein interactions in *Streptococcus pneumoniae* D39. Molecular microbiology 103:931-957.

33. Morlot C, Bayle L, Jacq M, Fleurie A, Tourcier G, Galisson F, Vernet T, Grangeasse C, Di Guilmi A-MJMm. 2013. Interaction of Penicillin-Binding Protein 2x and Ser/Thr protein kinase StkP, two key players in *Streptococcus pneumoniae* R6 morphogenesis. Molecular microbiology 90:88-102.

34. Myrbråten IS, Wiull K, Salehian Z, Håvarstein LS, Straume D, Mathiesen G, Kjos MJm. 2019. CRISPR Interference for Rapid Knockdown of Essential Cell Cycle Genes in *Lactobacillus plantarum*. mSphere 4:e00007-19.

35. Berg KH, Biørnstad TJ, Straume D, Håvarstein LS. 2011. Peptide-regulated gene depletion system developed for use in *Streptococcus pneumoniae*. Journal of bacteriology 193:5207-5215.

36. Hirschfeld C, Gómez-Mejia A, Bartel J, Hentschker C, Rohde M, Maaß S, Hammerschmidt S, Becher D. 2019. Proteomic Investigation Uncovers Potential Targets and Target Sites of Pneumococcal Serine-Threonine Kinase StkP and Phosphatase PhpP. Frontiers in Microbiology 10.

37. Sun X, Ge F, Xiao C-L, Yin X-F, Ge R, Zhang L-H, He Q-Y. 2009. Phosphoproteomic analysis reveals the multiple roles of phosphorylation in pathogenic bacterium *Streptococcus pneumoniae*. Journal of proteome research 9:275-282.

38. Karimova G, Pidoux J, Ullmann A, Ladant D. 1998. A bacterial two-hybrid system based on a reconstituted signal transduction pathway. Proceedings of the National Academy of Sciences 95:5752-5756.

39. Wu ZC, de Keyzer J, Berrelkamp-Lahpor GA, Driessen AJ. 2013. Interaction of *Streptococcus mutans* YidC1 and YidC2 with translating and nontranslating ribosomes. Journal of bacteriology 195:4545-4551.

40. Steinberg R, Knüpffer L, Origi A, Asti R, Koch H-G. 2018. Co-translational protein targeting in bacteria. FEMS microbiology letters 365:fny095.

41. Shiomi D, Sakai M, Niki H. 2008. Determination of bacterial rod shape by a novel cytoskeletal membrane protein. The EMBO journal 27:3081-3091.

42. Kjos M, Aprianto R, Fernandes VE, Andrew PW, van Strijp JA, Nijland R, Veening J-W. 2015. Bright fluorescent *Streptococcus pneumoniae* for live-cell imaging of host-pathogen interactions. Journal of bacteriology 197:807-818.

43. Bohrhunter JL, Rohs PD, Torres G, Yunck R, Bernhardt TG. 2020. MltG activity antagonizes cell wall synthesis by both types of peptidoglycan polymerases in *Escherichia coli*. Molecular Microbiology. ePub. https://doi.org/10.1111/mmi.14660.

44. Lacks S, Hotchkiss RD. 1960. A study of the genetic material determining an enzyme activity in pneumococcus. Biochimica et biophysica acta 39:508-518.

45. Higuchi R, Krummel B, Saiki R. 1988. A general method of in vitro preparation and specific mutagenesis of DNA fragments: study of protein and DNA interactions. Nucleic acids research 16:7351-7367.

46. Sung C, Li H, Claverys J, Morrison D. 2001. An *rpsL* cassette, janus, for gene replacement through negative selection in *Streptococcus pneumoniae*. Applied and environmental microbiology 67:5190-5196.

47. Johnsborg O, Eldholm V, Bjørnstad ML, Håvarstein LS. 2008. A predatory mechanism dramatically increases the efficiency of lateral gene transfer in *Streptococcus pneumoniae* and related commensal species. Molecular microbiology 69:245-253.

48. Ducret A, Quardokus EM, Brun YV. 2016. MicrobeJ, a tool for high throughput bacterial cell detection and quantitative analysis. Nat Microbiol. 1:16077

49. Johnsborg O, Håvarstein LS. 2009. Pneumococcal LytR, a protein from the LytR-CpsA-Psr family, is essential for normal septum formation in *Streptococcus pneumoniae*. Journal of bacteriology 191:5859-5864.

50. Straume D, Stamsås GA, Berg KH, Salehian Z, Håvarstein LS. 2017. Identification of pneumococcal proteins that are functionally linked to penicillin-binding protein 2b (PBP2b). Molecular microbiology 103:99-116.

Supplementary information

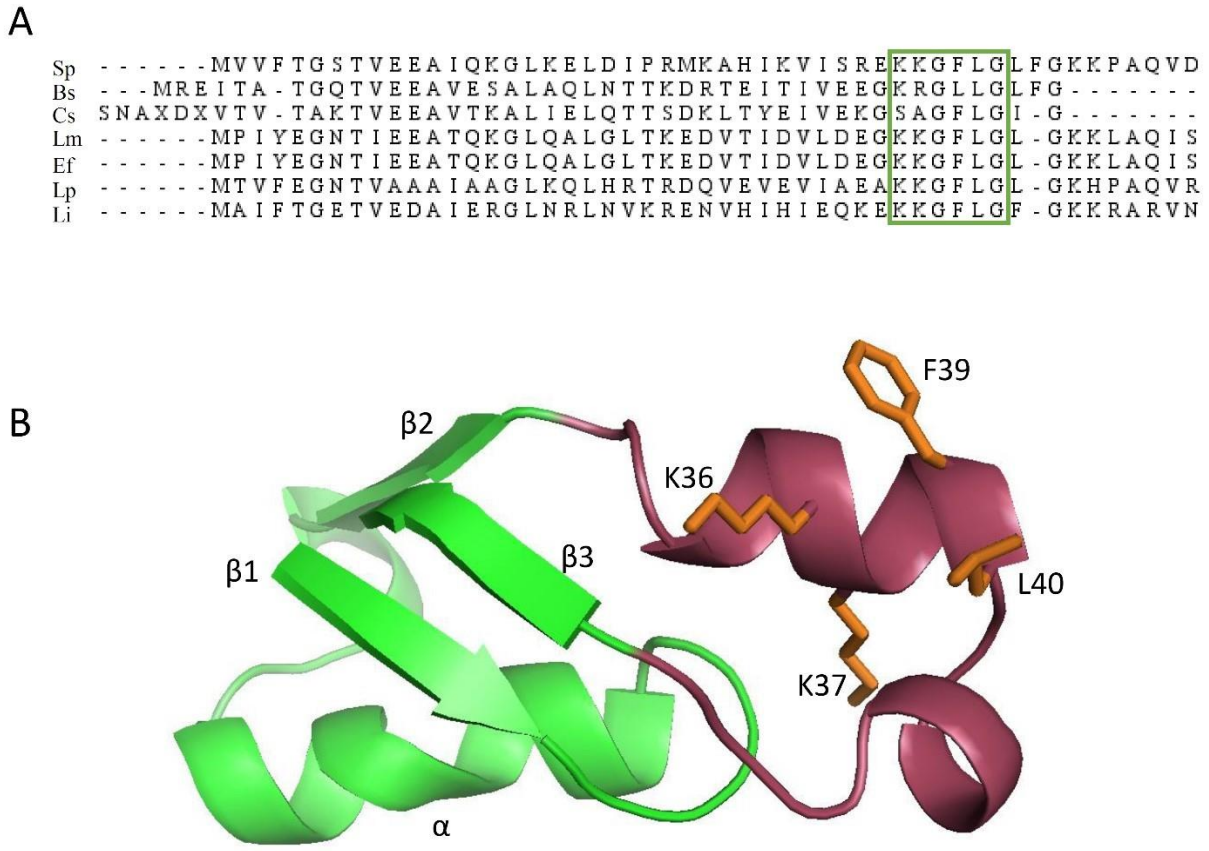

Fig. S1. A) Alignment of the Jag domains from (listed in same order as they appear in image) *S. pneumoniae* (AAL00654), *B. subtilis* (WP_158324121.1), *C. symbiosium* (3GKU_A), *Listeria monocytogenes* (EAC5385728.1), *Enterococcus faecalis* (WP_002403982.1), *Lactobacillus plantarum* (CCC80632.1), and *Lactococcus lactis* (WP_153242024.1). The conserved KKGFLG (green box) is indicated. B) Predicted structure (iTasser) of the Jag domain of *S. pneumoniae* EloR. The β-α-β-β fold with the α-helix laying on top of a three-stranded β-sheet is portrayed in green. The loop connecting the second and third β-strand is portrayed in red. The KKGFLG motif is shown in orange sticks.

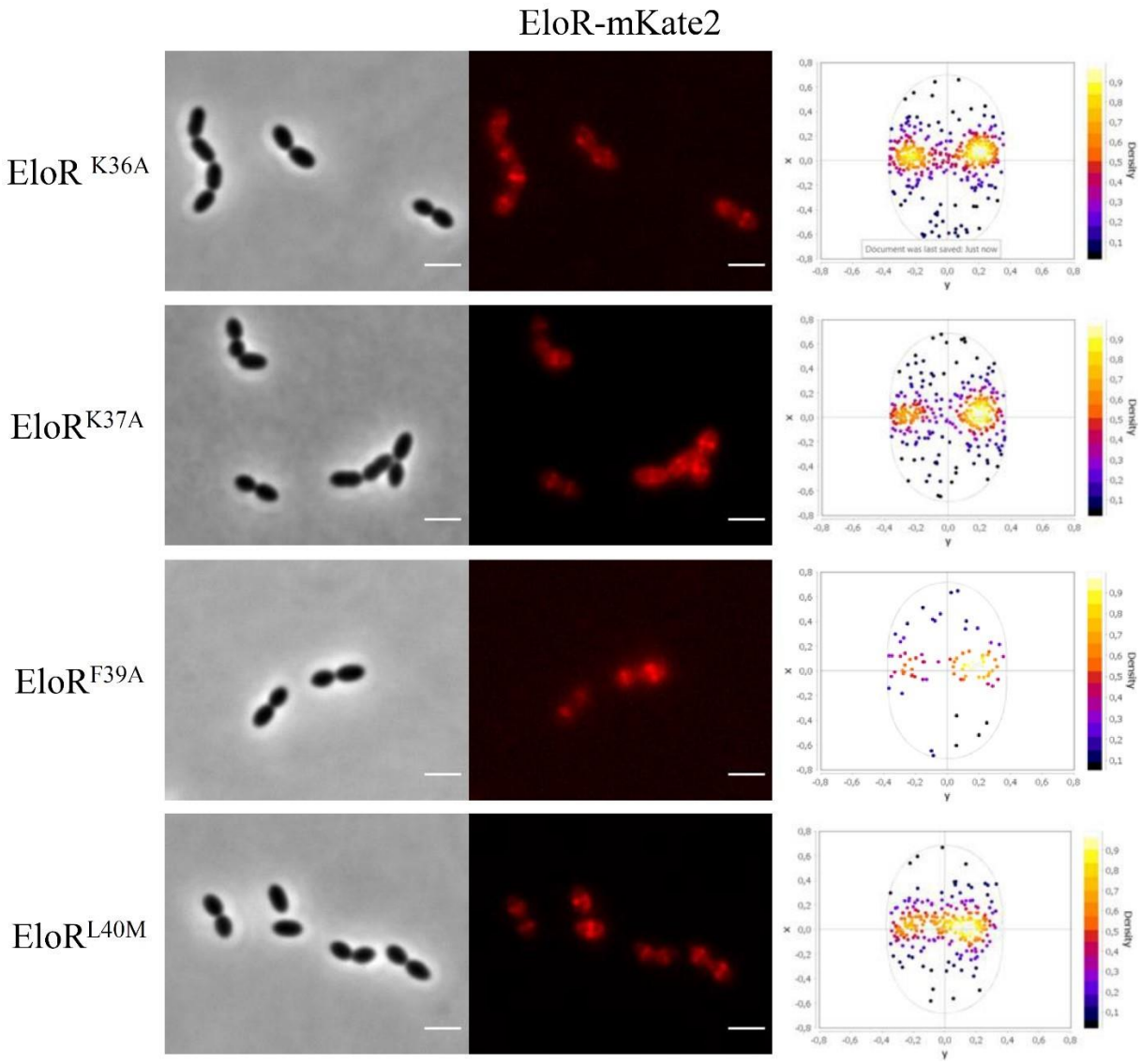

Fig. S2. Localization of EloR-mKate2 harboring the amino acid substitutions K36A, K37A, F39A and L40M. Microscopy images and corresponding focus density plots of detected foci are shown. x and y in the focus density plots denote the relative length - and width-axis, respectively. EloR-mKate2 is found concentrated at midcell with all the introduced mutations. The number of cells analyzed were N = 188 for K36A, N = 183 for K37A, N = 182 for F39A and N = 189 for L40M. Scale bars are 2 µm.

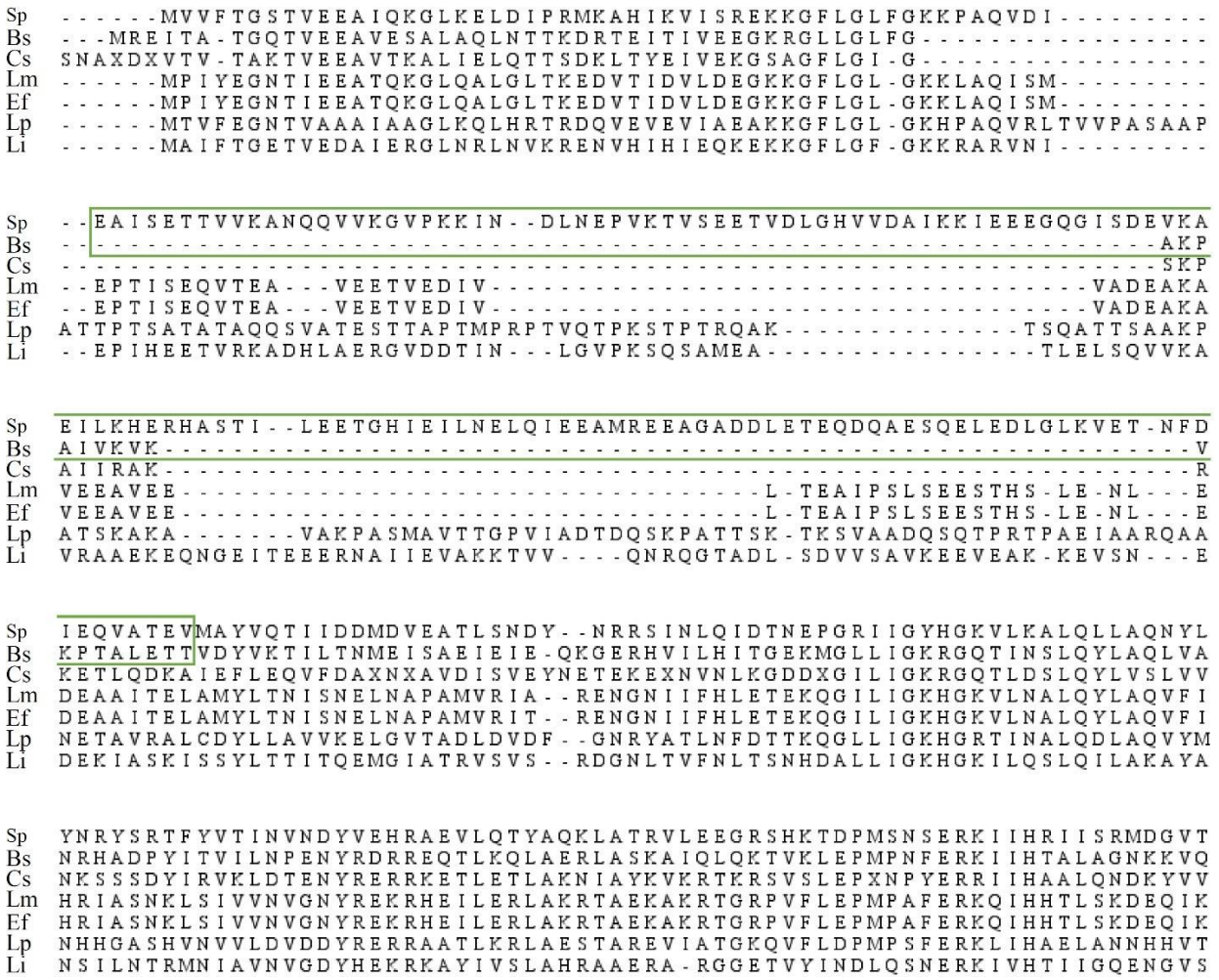

Fig. S3. Alignment of EloR from (listed in same order as they appear in image) *S. pneumoniae*, *B. subtilis*, *C. symbiosium*, *Listeria monocytogenes*, *Enterococcus faecalis*, *Lactobacillus plantarum*, and *Lactococcus lactis* (accession numbers are the same as in Fig. S1). The linker domain of EloR from *S. pneumoniae* (green box) is made up of approximately 135 amino acids, while the equivalent domain from *B. subtilis* (green box) only consists of approximately 10 amino acids.

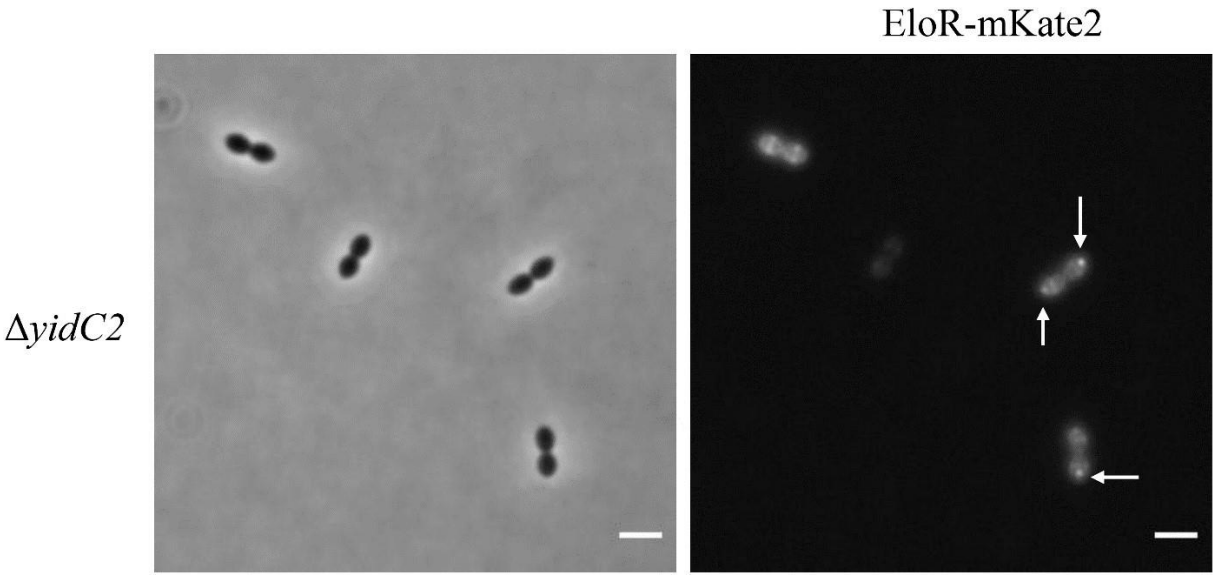

Fig. S4. Polar localized EloR-mKate2 in a Δ*yidC2* mutant is typically found in old cell poles as seen indicated by white arrows. Scale bars are 2 µm.

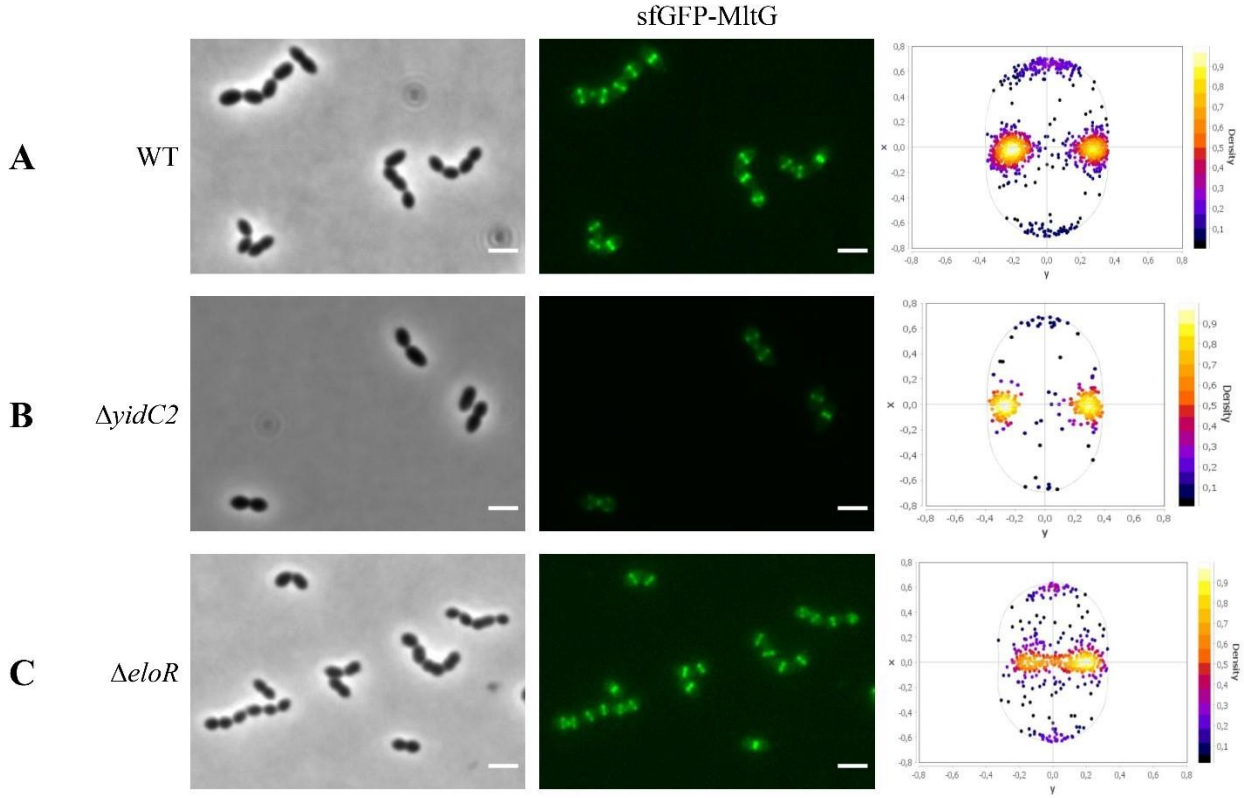

Fig. S5. Localization of sfGFP-MltG in a A) wild type background (N=1209), B) Δ*yidC2* mutant (N=253), and C) Δ*eloR* mutant (N=465). Microscopy images and corresponding focus density plots of detected foci are shown. N indicates the number of cells analyzed for each strain. x and y in the focus density plots denote the relative length- and width-axis, respectively. sfGFP-MltG was found localized at midcell in all genetic backgrounds investigated. Scale bars are 2 µm.

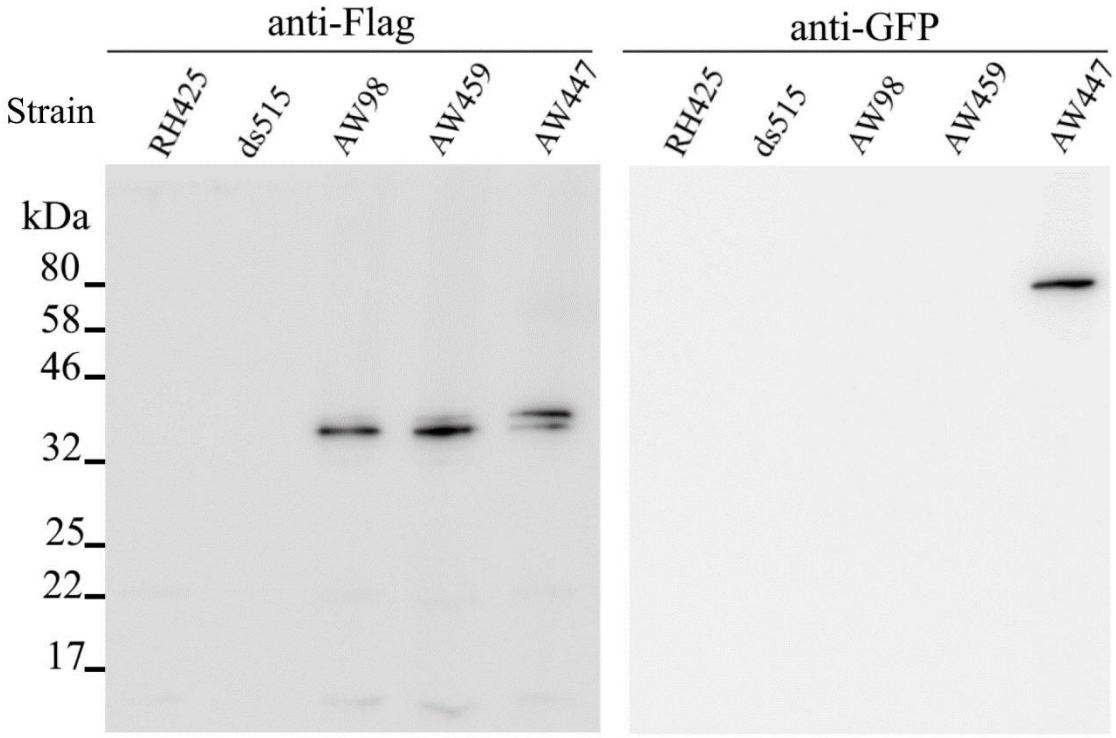

Fig. S6. Uncropped images of the immunoblots shown in Fig. 4 with protein size marker indicated.

Table S1. Primers.

Primer name	Sequence (5' → 3')	Reference
Primers used to create the *eloR-mKate2* amplicon, place it behind P_{comX} and screen		
DS433	ATTTATATTTATTATTGGAGGTTCAGTGGTAGTATTTAC AGGTTCAAC	This work
AW236	CTTCTCCACCAGATCCGGATTCTGTATCTACAACAACAT AGCG	This work
AW234	TCCGGATCTGGTGGAGAAG	This work
AW249	ATTGGGAAGAGTTACATATTAGAAATTAACGGTGTCCC AATTTACTAG	This work
KHB31	ATAACAAATCCAGTAGCTTTGG	(1)
KHB36	TGAACCTCCAATAATAAATATAAAT	(1)
KHB33	TTTCTAATATGTAACTCTTCCCAAT	(1)
KHB34	CATCGGAACCTATACTCTTTTAG	(1)
Primers used to create the *jag-mKate2* amplicon, place it behind P_{comX} and screen		
DS433	ATTTATATTTATTATTGGAGGTTCAGTGGTAGTATTTAC AGGTTCAAC	This work

AW238	CTTCTCCACCAGATCCGGATTTGACAACAGTCGTTTCACTAAT	This work
AW234	TCCGGATCTGGTGGAGAAG	This work
AW249	ATTGGGAAGAGTTACATATTAGAAATTAACGGTGTCCCAATTTACTAG	This work
KHB31	ATAACAAATCCAGTAGCTTTGG	(1)
KHB36	TGAACCTCCAATAATAAATATAAAT	(1)
KHB33	TTTCTAATATGTAACTCTTCCCAAT	(1)
KHB34	CATCGGAACCTATACTCTTTTAG	(1)
Primers used to create the *jag-linker-mKate2* amplicon, place it behind P_{comX} and screen		
DS433	ATTTATATTTATTATTGGAGGTTCAGTGGTAGTATTTACAGGTTCAAC	This work
AW240	CTTCTCCACCAGATCCGGATTGTTCAATATCAAAGTTCGTTTCAA	This work
AW234	TCCGGATCTGGTGGAGAAG	This work
AW249	ATTGGGAAGAGTTACATATTAGAAATTAACGGTGTCCCAATTTACTAG	This work
KHB31	ATAACAAATCCAGTAGCTTTGG	(1)
KHB36	TGAACCTCCAATAATAAATATAAAT	(1)
KHB33	TTTCTAATATGTAACTCTTCCCAAT	(1)
KHB34	CATCGGAACCTATACTCTTTTAG	(1)
Primers used to create the *linker-mKate2* amplicon, place it behind P_{comX} and screen		
AW239	GAAATAAATAAGGAGGAATCTGGTAGTGGCAAATCAACAGGTAGTAA	This work
AW240	CTTCTCCACCAGATCCGGATTGTTCAATATCAAAGTTCGTTTCAA	This work
AW234	TCCGGATCTGGTGGAGAAG	This work
AW249	ATTGGGAAGAGTTACATATTAGAAATTAACGGTGTCCCAATTTACTAG	This work
KHB31	ATAACAAATCCAGTAGCTTTGG	(1)
KHB36	TGAACCTCCAATAATAAATATAAAT	(1)
KHB33	TTTCTAATATGTAACTCTTCCCAAT	(1)
KHB34	CATCGGAACCTATACTCTTTTAG	(1)
Primers used to create the *hlpA-gfp-chloramphenicol* amplicon		
MK180	AACAAGTCAGCCACCTGTAG	(2)
MK181	CGTGGCTGACGATAATGAGG	(2)
Primers used to create the *flag-eloR* amplicon		
DS374	CGAAACCTTGGGATACGCAG	(3)
DS377	CAGCACCCACGTTAAGCAAC	(3)
Primers used to create the Δ*stkP*::janus amplicon		
KHB410	AGAAATATTAGGTAGTGTTTGTC	(4)

KHB411	CCAGACAGTCATGCCCAAAATC	(4)
Primers used to create the Δ*rodZ*::janus amplicon		
KHB445	TAGATTTACTTGATGAATTGGTAA	(4)
KHB448	CCACACGTTGCTTTTGGCC	(4)
Primers used to create the Δ*yidC2*::janus amplicon		
DS403	ATATTGATCCAGCTATCATTCC	This work
DS404	CACATTATCCATTAAAAATCAAACTTCCTTCCCGGTAA ATCTTTG	This work
DS405	GTCCAAAAGCATAAGGAAAGATAAGGAGGAATCTGGT AGTG	This work
DS406	GCTCATCACCTTCAGAGTAAC	This work
Primers used to create the Δ*eloR*::janus amplicon		
DS374	CGAAACCTTGGGATACGCAG	(3)
DS377	CAGCACCCACGTTAAGCAAC	(3)
Primers used to create the P_{comX}-*eloR*^{K36A}-*mKate2* amplicon		
AW258	GCAAAAGGCTTTCTTGGTCTATTTGG	This work
AW259	CCAAATAGACCAAGAAAGCCTTTTGCCTCCCTAGAAAT GACTTTGATATG	This work
KHB31	ATAACAAATCCAGTAGCTTTGG	(1)
KHB34	CATCGGAACCTATACTCTTTTAG	(1)
Primers used to create the P_{comX}-*eloR*^{K37A}-*mKate2* amplicon		
AW260	GCAGGCTTTCTTGGTCTATTTGGTA	This work
AW261	TACCAAATAGACCAAGAAAGCCTGCTTTCTCCCTAGAA ATGACTTTGAT	This work
KHB31	ATAACAAATCCAGTAGCTTTGG	(1)
KHB34	CATCGGAACCTATACTCTTTTAG	(1)
Primers used to create the P_{comX}-*eloR*^{F39A}-*mKate2* amplicon		
AW262	GCACTTGGTCTATTTGGTAAAAAACCA	This work
AW263	TGGTTTTTTACCAAATAGACCAAGTGCGCCTTTTTTCTC CCTAGAAATGA	This work
KHB31	ATAACAAATCCAGTAGCTTTGG	(1)
KHB34	CATCGGAACCTATACTCTTTTAG	(1)
Primers used to create the P_{comX}-*eloR*^{L40M}-*mKate2* amplicon		
AW266	ATGGGTCTATTTGGTAAAAAACCAGC	This work
AW267	GCTGGTTTTTTACCAAATAGACCCATAAAGCCTTTTTTC TCCCTAGAAAT	This work
KHB31	ATAACAAATCCAGTAGCTTTGG	(1)
KHB34	CATCGGAACCTATACTCTTTTAG	(1)
Primers used to introduce *jag-linker* into BACTH plasmids pKT25		
AW271	GATCTCTAGAGGTAGTATTTACAGGTTCAACTGTT	This work
AW272	GTACGAATTCTTATTTGACAACAGTCGTTTCACTAAT	This work
Primers used to introduce *jag* into BACTH plasmids pKT25		

AW113	GATCTCTAGAGGTAGTATTTACAGGTTCAACTGTT	This work
AW116	GATCGAATTCGATTCAATATCCACTTGGGCTGG	This work
Primers used to introduce *mltGcyt* into BACTH plasmids and pUT18C		
AW268	GATCTCTAGAGTTGAGTGAAAAGTCAAGAGAAGAA	This work
AW269	GATCGAATTCTTAGAATGAAATCACAAAAGCTTTCAC	This work
Primers used to introduce *mltGcytΔDUF* into BACTH plasmids pUT18C		
MLH1	GCTATGATGAAGTTCTGAAAGAAGAAACACCTACGCCTGCTAC	This work
MLH2	TCTTTCAGAACTTCATCATAGC	This work
AW268	GATCTCTAGAGTTGAGTGAAAAGTCAAGAGAAGAA	This work
AW269	GATCGAATTCTTAGAATGAAATCACAAAAGCTTTCAC	This work
Primers used to introduce *mreD* into BACTH plasmid pKT25 and pUT18C		
KHB455	TACGAAGCTTG ATGAGACAGTTGAAGCGAGTT	This work
GS336	TACGGAATTCGATAGATAATATTTTTCAAAAATAAATTG	This work
Primers used to introduce *yidC2* into BACTH plasmid pKT25 and pUT18C		
MK19	GAGCGGATCCCGGAGTGAAAAAGAAACTAAAGTTG	This work
MK20	GCATGAATTCGAACCAGAACCACCTTTCGTTTTCTGAGCCTTTTTCTTG	This work

References.

1. Berg KH, Biørnstad TJ, Straume D, Håvarstein LS. 2011. Peptide-regulated gene depletion system developed for use in *Streptococcus pneumoniae*. Journal of bacteriology 193:5207-5215.

2. Kjos M, Aprianto R, Fernandes VE, Andrew PW, van Strijp JA, Nijland R, Veening J-W. 2015. Bright fluorescent *Streptococcus pneumoniae* for live-cell imaging of host-pathogen interactions. Journal of bacteriology 197:807-818.

3. Stamsås GA, Straume D, Ruud Winther A, Kjos M, Frantzen CA, Håvarstein LS. 2017. Identification of EloR (Spr1851) as a regulator of cell elongation in *Streptococcus pneumoniae*. Molecular microbiology 105:954-967.

4. Straume D, Stamsås GA, Berg KH, Salehian Z, Håvarstein LS. 2017. Identification of pneumococcal proteins that are functionally linked to penicillin-binding protein 2b (PBP2b). Molecular microbiology 103:99-116.